ACS OMEGA

http://pubs.acs.org/journal/acsodf

Article

Paraverrucsins A−F, Antifeedant, and Antiphytopathogenic Polyketides from Rhizospheric *Paraphaeosphaeria verruculosa* and Induced Bioactivity Enhancement by Coculturing with Host Plant *Dendrobium officinale*

Ming Hu,[§] Xue-Qiong Yang,[§] Cui-Fang Wang, Tong-De Zhao, Dai-Li Wang, Ya-Bin Yang,* and Zhong-Tao Ding*

Cite This: *ACS Omega* 2020, 5, 30596−30602

Read Online

ACCESS | Metrics & More | Article Recommendations | Supporting Information

ABSTRACT: Six new polyketides named paraverrucsins A−F (**1**−**6**) with oxabicyclic and dioxatricyclic skeletons, together with eight known metabolites (**7**−**14**), were discovered and isolated from the fermentation medium of *Paraphaeosphaeria verruculosa*. Paraverrucsin A−C possessed a novel decarboxylated skeleton compared with that of trichocladinols. Their structures were elucidated by extensive spectral analysis and DP4+ calculations. Paraverrucsins B/C and D/E were isolated as a mixture for the mutarotation occurred at C-2. Paraverrucsins B/C, D/E, F/trichocladinol B, **8**, and **9** displayed antifeedant activities against silkworm larvae, with antifeedant index percentages ranging from 62.5 to 93.0%, at a concentration of 50 $\mu g/cm^2$. Among them, Paraverrucsins B/C and **9** had EC_{50} values at 13.9 and 18.2 $\mu g/cm^2$. Most compounds showed antifungal activities against phytopathogenic fungi with minimum inhibitory concentration (MIC) values of 16−64 $\mu g/mL$. Coculture of *P. verruculosa* and host plant *Dendrobium officinale* leads to the enhancement of antifeedant and antiphytopathogenic activities. Compounds **1**, **2**/**3**, **4**/**5**, **6**/**14** were tested for cytotoxicity against five human carcinoma cell lines, HL-60, A549, MCF-7, SW480, and SMMC-7721, while they exhibited selected cytotoxicity against SW480 with inhibition ratios of 32−38% at a concentration of 40 μM.

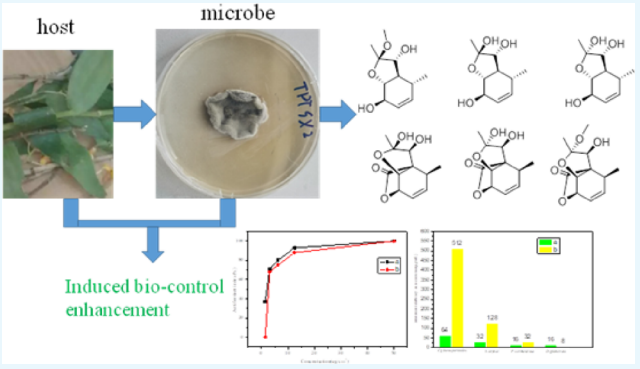

INTRODUCTION

In recent years, negative impacts on the environment and on human health were caused by the application of synthetic insecticides.[1] Biological control agents (BCA) have become a promising alternative to chemical pesticides for disease control in crop plant.[2] Numerous rhizosphere fungi isolates have the inhibition against the growth of the plant-pathogenic fungi, stimulation of plant growth and defense, and resistance to insect herbivores.[3−5] Hence, rhizospheric microorganisms are considered as good BCA candidates for controlling plant diseases. *Paraphaeosphaeria* sp. had been regarded as pathogenic fungi.[6] Previous works led to many new metabolites from *Paraphaeosphaeria* sp. TR-022.[7] In this research, new antifungal and antifeedant metabolites from rhizospheric *Paraphaeosphaeria verruculosa* were identified (Figure 1). The plant−microbe interaction can induce the productions of plant growth promoters and pharmaceuticals.[8] However, a few was reported about the inducing metabolites with biocontrol activity by the coculture of plant−microbe. The compound isolations, structure elucidation, bioactivities, and the inducing bioactivity enhancement by coculture of plant−microbe were described in this paper.

RESULTS AND DISCUSSION

Structural Elucidation. Compound **1** was assigned the molecular formula $C_{11}H_{18}O_4$ by HR-ESIMS, indicating three degrees of unsaturation. The ^1H and ^{13}C NMR spectroscopic analyses, including distortionless enhancement by polarization transfer (DEPT) clearly showed two methyls, seven methines (three *O*-methines and two protonated olefinic carbons), one methoxyl, and a doubly oxygenated carbon (δ_C: 109.8) (Table 1). Two olefinic carbons accounted for one degree of unsaturation, while the remaining two degrees of unsaturation suggested the presence of a bicyclic structure. According to

Received: September 16, 2020
Accepted: November 5, 2020
Published: November 17, 2020

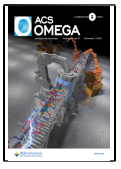

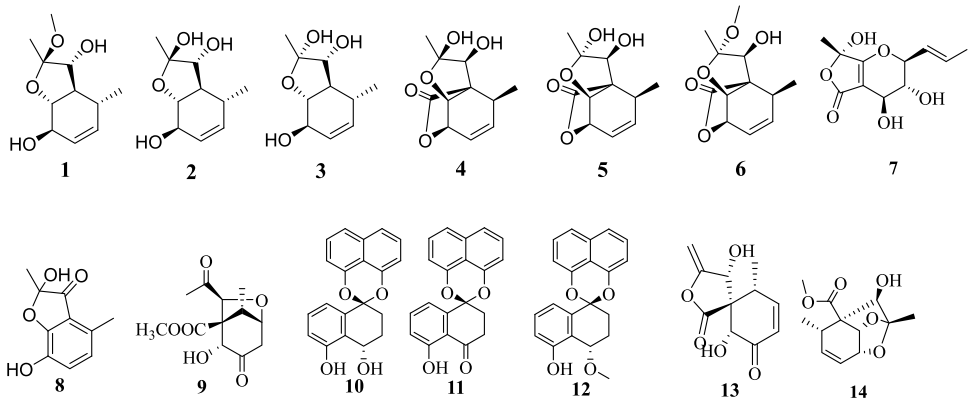

Figure 1. Structures of compounds from *Paraphaeosphaeria verruculosa*.

Table 1. ^{13}C NMR and ^{1}H NMR Data of Compounds 1−3 in MeOD (δ in ppm, J in Hz)

	1		2		3	
pos.	δ_H	δ_C	δ_H	δ_C	δ_H	δ_C
1						
2		109.8		106.4		101.8
3	3.82, d (8.5)	82.5	3.94, d (8.5)	83.0	3.72, d (10.4)	79.3
4	1.29, m	53.8	1.40, m	53.6	1.68, m	50.0
5	3.38, dd (8.0, 3.5)	79.8	3.65, dd (8.0, 3.6)	79.3	3.37, dd (8.2, 3.3)	79.7
6	4.14, m	71.5	4.20, m	71.7	4.26, m	72.3
7	5.34, dt (9.9, 2.2)	128.4	5.45, dt (9.5, 1.8)	128.4	5.45, dt (9.5, 1.8)	128.5
8	5.41, dt (9.9, 2.0)	134.8	5.53, m	134.8	5.53, m	135.0
9	2.20, m	35.7	2.34, m	35.7	2.30, m	35.9
10	1.22, s	17.5	1.38, s	22.6	1.45, s	24.3
11	1.02, d (7.2)	18.2	1.14, d (7.1)	18.1	1.17, d (6.9)	18.2
OCH_3	3.21, s	47.6				

these data, the structure of compound **1** showed a similar skeleton to trichocladinol D.[9] Compound **1** had one more methoxyl but nonexistence of γ-lactone ring. The presence of a cyclohexene ring was determined by the heteronuclear multiple bond correlation (HMBC) correlations from H-5 to C-6; H-8 to C-4, C-6, and C-9; and H-11 to C-4, C-8, and C-9, and ^{1}H-^{1}H COSY correlations of H-3/H-4/H-5/H-6, H-7/H-8, and H-9/H-11 also confirmed this structure (Figure 2). Moreover, the other HMBC correlations from H-3 to C-2 and C-9; and H-10 to C-2 and C-3 confirmed the tetrahydrofuran (THF) ring. The methoxyl connected to C-2 was determined

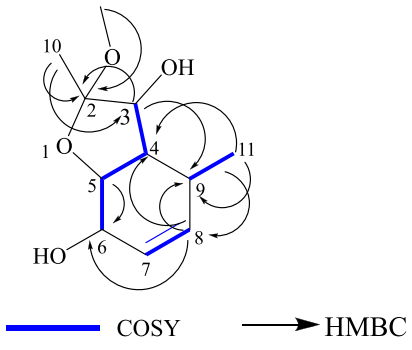

Figure 2. Key ^{1}H-^{1}H COSY and HMBC correlations of compound **1**.

by the HMBC correlations from OCH_3 to C-2. On the basis of the NMR data, the planar structure of **1** was established, as shown in Figure 1. The relative configurations of **1a**, **1b**, and **1c** were observed by employing calculations of shielding tensor values with support from DP4+ probability analysis. The theoretical calculations of ^{1}H and ^{13}C NMR chemical shifts of three possible isomers (2*R*, 3*S*, 4*R*, 5*S*, 6*S*, 9*S*)-**1a**, (2*R*, 3*R*, 4*R*, 5*R*, 6*R*, 9*R*)-**1b**, and (2*S*, 3*S*, 4*R*, 5*S*, 6*S*, 9*S*)-**1c** were predicted using the GIAO method at the PCM/mPW1PW91/6−311 + G (d, p) level of theory. The theoretical calculations of NMR chemical shifts were compared with the experimental data (Table 1) using linear correlation and the DP4 + method; the result showed that the isomer **1b** was the most reasonable structure. Paraverrucsin A (**1**) possessed a novel decarboxylated skeleton compared with that of trichocladinols.

Compounds **2** and **3** were isolated as a mixture of diastereoisomers in a 1:1 ratio. The ^{1}H NMR and ^{13}C NMR data of **2** and **3**, with the help of the molecular formula $C_{10}H_{16}O_4$ deduced by HR-ESIMS, revealed the similar structure as **1** except for a missing methoxyl. The NMR spectra were almost identical for compounds **2** and **3**, except that the chemical shift values for the C-2, C-3, C-4, and C-10 in **2** (δ_H/δ_C: 106.4, 3.94/83.0, 1.40/53.6, and 1.38/22.6) were different from those in **3** (δ_H/δ_C: 101.8, 3.72/79.8, 1.68/50.0, and 1.45/24.6). The structures of compounds **2** and **3** were confirmed by the COSY correlations of H-3/H-4/H-5/H-6; H-7/H-8 and H-9/H-11 and HMBC correlations from H-3 to C-2, C-4, and C-9 in compound **2**; H-3 to C-9 and C-10 in compound **3**; H-5 to C-6; H-8 to C-4, C-6, and C-9; H-11 to C-4, C-8, and C-9 (Figure 3). The relative configurations of **2** and **3** were determined using the NOESY spectrum (Figure 3) and DP4+ probability analysis. The NOESY correlations of H-3/H-9, H-3/H-10, H-4/H-6, and H-5/H-9 in **2** and **3** indicated that the possible relative configurations of **2** and **3** are (2*S*, 3*S*, 4*R*, 5*S*, 6*S*, 9*S*)-**2a**, (2*R*, 3*R*, 4*R*, 5*R*, 6*R*, 9*R*)-**2b**, (2*R*, 3*S*, 4*R*, 5*S*, 6*S*, 9*S*)-**3a**, and (2*S*, 3*R*, 4*R*, 5*R*, 6*R*, 9*R*)-**3b**. Furthermore, NMR data of possible isomers calculated by using the DP4+ probability analysis (Table 1) and the linear correlation indicated that **2b** and **3b** were the most reasonable configurations. Therefore, the structures of **2** and **3** were as shown in Figure 1 and named as paraverrucsin B and C.

Compounds **4** and **5** and were isolated as a mixture in a 1:1 ratio. The molecular formulas of **4** and **5** were determined to be $C_{11}H_{14}O_5$ by the analysis of its HR-ESIMS spectrum, indicating five degrees of unsaturation. Two olefinic carbons and one carbonyl account for two degrees of unsaturation, while the remaining three degrees of unsaturation indicated the

https://dx.doi.org/10.1021/acsomega.0c04548
ACS Omega 2020, 5, 30596−30602

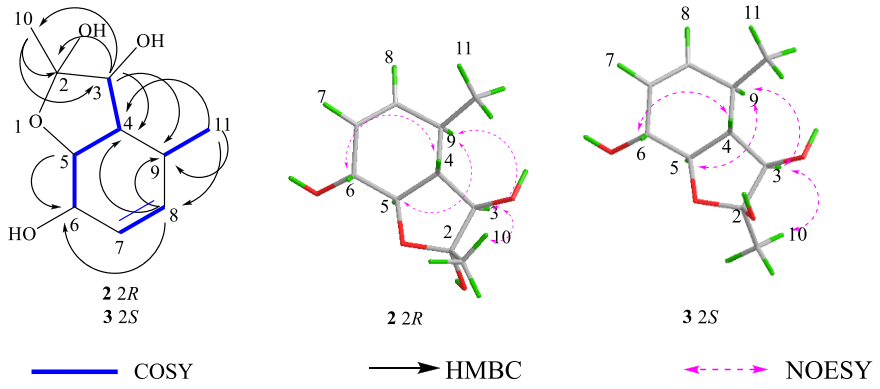

Figure 3. Key ^{1}H-^{1}H COSY, HMBC, and NOESY correlations of compounds **2** and **3**.

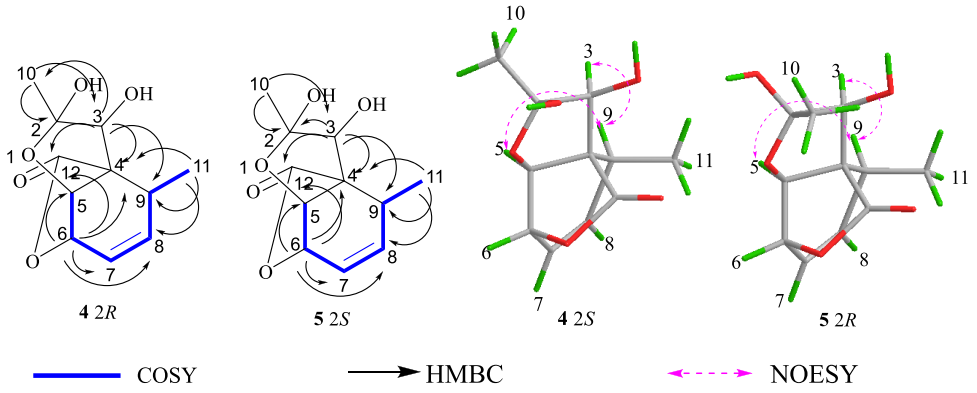

Figure 4. Key ^{1}H-^{1}H COSY, HMBC, and NOESY correlations of compounds **4** and **5**.

presence of a tricyclic in compounds **4** and **5**. Furthermore, the ^{1}H and ^{13}C NMR spectroscopic analyses clearly showed a similar structure as **1** and trichocladinols,[9] expect for the existence of γ-lactone ring in compounds **4** and **5**. The γ-lactone ring connected to C-4 and C-6 were confirmed by the HMBC correlations from H-3 to C-4, C-9, C-10, and C-12 in **4**; H-3 to C-2, C-4, C-9, and C-12 in **5**; H-6 to C-4, C-5, C-7, C-8, and C-12 (Figure 4). The structures of compounds **4** and **5** was also determined by the HMBC correlations from H-10 to C-2 and C-3; and H-11 to C-4, C-8, and C-9 (Figure 3). Also, the COSY correlations of H-5/H-6/H-7/H-8/H-9/H-11 also construct this structural fragment. The relative configurations of **4** and **5** were also determined using NOESY correlations of H-3/H-9 and H-5/H-9 in **4** and **5** and the DP4+ probability analysis (Figure 4). The DP4+ probability analysis of NMR data of five possible isomers by using the linear correlation showed that (2*R*, 3*S*, 4*R*, 5*S*, 6*R*, 9*S*)-**4c** and (2*S*, 3*S*, 4*R*, 5*S*, 6*R*, 9*S*)-**5c** were the most reasonable configurations. The separation of mixtures **2**/**3** and **4**/**5** were carried on silica gel and Lichroprep RP-18, but it cannot be segregated. The reason might be the mutarotation that occurred at C-2.

Compound **6** and trichocladinol B (**14**) were isolated as a mixture in a 1:1 ratio. Trichocladinol B was identified by comparing the NMR data with those already published.[10] The molecular formula of compound **6** was determined to be $C_{12}H_{16}O_5$ by the analysis of its HR-ESIMS spectrum and NMR data. Analysis of ^{1}H and ^{13}C NMR spectroscopic data (Table 2) of **6** revealed nearly identical structural features found in **4** and **5**, except for one more oxygenated methyl in **6**. According to the HMBC correlation from OCH_3 to C-2, it suggested that the methoxyl is connected to C-2 (Figure 5). The COSY correlations of H-5/H-6/H-7/H-8/H-9/H-11 and HMBC correlations from H-3 to C-4, C-9, and C-12; H-5 to C-6, C-9, and C-12; H-8 to C-4; H-11 to C-4, C-8, and C-9; and H-10 to C-2 and C-3 confirmed the structure of **6**. Further detailed inspection of NMR spectra of **4**−**6** suggested the ^{13}C NMR data of **6** were more similar to those in **5**, which

Table 2. ^{13}C NMR and ^{1}H NMR Data of Compounds 4−6 (δ in ppm, J in Hz)[a,b]

	4[a]		**5**[a]		**6**[b]	
pos.	δ_H	δ_C	δ_H	δ_C	δ_H	δ_C
1						
2		103.2		108.0		111.4
3	4.15, s	80.9	4.32, s	85.0	4.12, s	85.3
4		55.7		57.7		57.3
5	4.40, s	81.5	4.22, s	82.3	4.15, s	81.6
6	4.74, d (5.8)	74.7	4.72, d (5.8)	74.3	4.72, d (6.0)	74.3
7	6.15, m	126.3	6.18, m	125.7	6.08, m	126.0
8	5.80, dd (9.4, 2.4)	137.7	5.86, dd (9.4, 2.5)	137.6	5.76, dd (9.1, 2.6)	138.0
9	2.85, m	39.2	2.87, m	38.8	2.80, m	38.5
10	1.50, s	24.5	1.36, s	22.6	1.15, s	17.9
11	1.23, d (6.9)	15.3	1.20, d (7.1)	15.5	1.03, d (7.3)	15.9
12		177.2		177.2		177.6
OCH_3					3.13, s	48.5

[a] ^{1}H recorded at 600 MHz and ^{13}C was recorded at 150 MHz in MeOD. [b] ^{1}H recorded at 600 MHz and ^{13}C recorded at 150 MHz in actone-d_6

https://dx.doi.org/10.1021/acsomega.0c04548
ACS Omega 2020, 5, 30596−30602

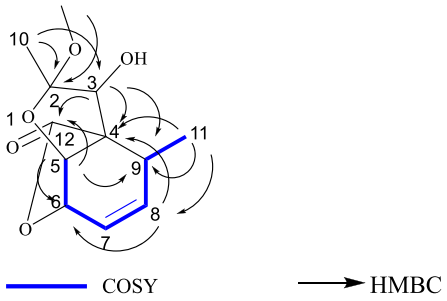

Figure 5. Key ^{1}H-^{1}H COSY and HMBC correlations of compound **6**.

indicated that the relative configuration of **6** might be identical to **5**. In addition, the DP4+ protocol was again applied to the calculations of ^{1}H and ^{13}C NMR chemical shifts of the five possible epimers. The statistical results indicated that the epimer **6c** was the correct structure for **6**.

The other known compounds were determined to be massarilactone D (**7**),[11] enalin A (**8**),[12] massarilactone G (**9**),[13] palmarumycin CJ-12,371 (**10**),[14] palmarumycin CP_2 (**11**),[15] palmarumycin CP_{19} (**12**),[16] massarigenin C (**13**),[17] and trichocladinol B (**14**).[10]

The Insect Antifeedant Activities. As shown in Table 3, compounds **2/3** and **9** were found to have potential deterrence against silkworm larvae, with EC_{50} values of 13.9 and 18.2 $\mu g/cm^2$. Other compounds also displayed insect antifeedant activities, with antifeedant index percentages ranging from 42.0 to 93.0%, at a concentration of 50 $\mu g/cm^2$. The positive control abamectin showed antifeedant activity with an EC_{50} value of 3.0 $\mu g/cm^2$. As shown in Figure 6, the extracts from the coculture of host plant *D. officinale* and *P. verruculosa* showed more antifeedant activity against silkworm larvae than that of extracts from *P. verruculosa.* Therefore, the synergism of the host plant *D. officinale* and *P. verruculosa* can induce the antifeedant activity.

Table 3. Insect Antifeedant Activity of Compounds 2/3, 4/5, 6/14, 7−13 against Silkworm Larvae

compounds	antifeedant index (%)	ED_{50} ($\mu g/cm^2$)
2/3	89.0	13.9
4/5	62.5	no test
6/14	92.0	no test
7	45.0	no test
8	86.0	no test
9	93.0	18.2
10	55.0	no test
11	42.5	no test
12	42.0	no test
13	51.5	no test
abamectin	94.0	3.0

Evaluation of the Antifungal Activities. As shown in Table 4, compounds **1−13** exhibited antifungal activity against four strains of plant pathogenic fungi (*Colletotrichum gloeosporioides*, *Didymella glomerata*, *Nigrospora oryzae*, and *Paraphaeosphaeria verruculosa*). Interestingly, compound **6/14** exhibited significant antifungal activities against *C. gloeosporioides* with an MIC of 8 $\mu g/mL$, which was better than that of the positive control nystatin. Compounds **6/14** and **12** showed antifungal activities against *D. glomerata* with MICs of 16 $\mu g/mL$, equivalent to that of the positive control. Compound **11** showed significant antifungal activities against *P. verruculosa* with an MIC of 8 $\mu g/mL$. As shown in Figure 7, extracts from the coculture of host plant *D. officinale* and *P. verruculosa*

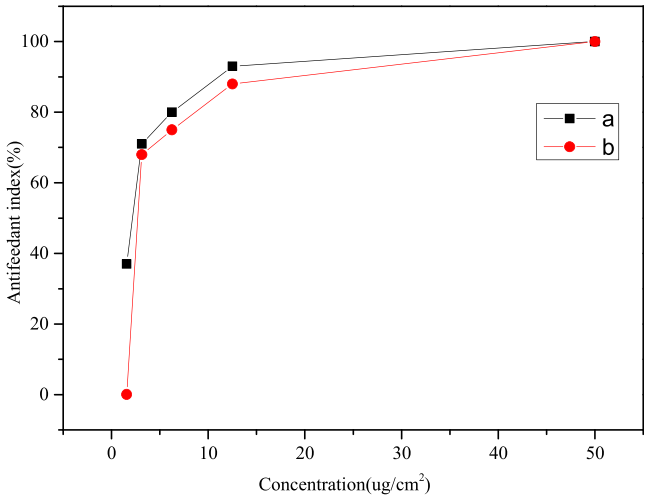

Figure 6. Antifeedant activities of *P. verruculosa* cultured in coculture (a: coculture of *P. verruculosa* and *D. officinale*) and monoculture (b: monoculture of *P. verruculosa*) against silkworm larvae.

Table 4. Antifungal Activities of Compounds 1, 2/3, 4/5, 6/14, 7−13 (MIC at $\mu g/mL$)

compounds	*C. gloeosporioides*	*D. glomerata*	*N. oryzae*	*P. verruculosa*
1	64	64	32	64
2/3	32	32	256	32
4/5	16	32	256	64
6/14	8	16	128	32
7	16	64	512	256
8	16	128	64	64
9	32	32	512	16
10	32	32	512	16
11	16	32	512	8
12	32	16	512	64
13	64	32	128	64
nystatin	16	16	16	16

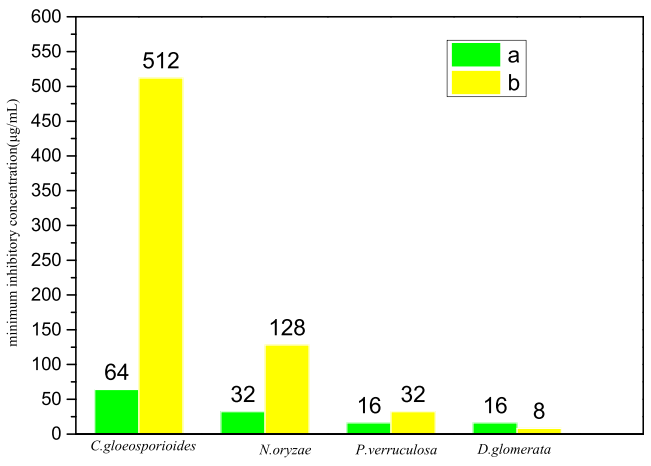

Figure 7. Antifungal activity of coculture (a: *P. verruculosa*−*D. officinale*) and monoculture of *P. verruculosa* (b: monoculture of *P. verruculosa*) against four phytopathogens (*C. gloeosporioides*, *D. glomerata*, *N. oryzae*, and *P. verruculosa*).

https://dx.doi.org/10.1021/acsomega.0c04548
ACS Omega 2020, 5, 30596−30602

showed more antiphytopathogenic activity against *C. gloeosporioides*, *N. oryzae*, and *P. verruculosa* than that of extracts from *P. verruculosa*. Therefore, the interaction of host plant *D. officinale* and *P. verruculosa* had an important induction on the antiphytopathogenic metabolite productions.

Evaluation of the Cytotoxicity. All new compounds were tested for cytotoxicity against five human carcinoma cell lines. Compounds **1**, **2**/**3**, **4**/**5**, and **6**/**14** showed selected weak cytotoxicity against SW480 with inhibition ratios of 32−38% at a concentration of 40 μM. All compounds indicated no obvious cytotoxicity against HL-60, A-549, SMMC-7721, and MCF-7 with inhibition ratios of 1−16, 2−3, 6−7, and 1−5% at a concentration of 40 μM. Cisplatin was used as a positive control with IC_{50} values of 1.06, 3.92, 10.89, 11.87, and 8.34 μM against HL-60, SMMC-7721, A-549, MCF-7, and SW480 cells, respectively.

MATERIALS AND METHODS

General Experimental Procedures. Silica gel (200−300 mesh, Qingdao Marine Chemical Group Co.), LiChroprep RP-18 (40−63 mm; Merck, Darmstadt, Germany), and Sephadex LH-20 (GE Healthcare Co.) were used for column chromatography. 1D and 2D NMR spectra were obtained on a Bruker AVANCE 400, 500, 600 MHz NMR instrument (Bruker, Karlsruhe, Germany). MS spectra were recorded with an Agilent G3250AA (Agilent, Santa Clara, U.S.A.) and an AutoSpec Premier P776 spectrometer (Waters, Milford, U.S.A.). Optical rotations (ORs) were obtained on a JASCO P-1020 polarimeter.

Fungus Material and Fermentation. The fungus was isolated by using a potato dextrose agar medium (PDA) (peeled and cut potato; 200 g/L, glucose 20 g/L, agar 15 g/L) from the rhizosphere of *D. officinale* in Wenshan of Yunnan Province. The species was identified as *P. verruculosa* by internal transcribed spacer (ITS) gene sequencing. The fungus has been preserved at the School of Chemical Science and Technology, Yunnan University, China. The pure strain was stored in 50% glycerol at −80 °C. *P. verruculosa* was maintained on the PDA medium. Small agar plugs (approximately 5 mm × 5 mm) of the fungus were cultured in 0.5 L Erlenmeyer flasks containing 100 mL of potato dextrose broth (PDB, potato infusion of 200 g fresh potato, 15 g dextrose, and 1.0 L distilled water, pH 7.0) at 130 rpm and 28 °C for 3 days. Each 20−25 mL of the seed culture was transferred into a 1.0 L Erlenmeyer flask containing 250 mL of PDB and incubated at 130 rpm and 28 °C for 7 days. Coculture of *P. verruculosa* and *D. officinale* was obtained according to the method described above (medium: 160 g potato, 40 g *D. officinale*, 15 g dextrose, and 1.0 L distilled water, pH 7.0).

Extraction and Isolation of Compounds. The production culture (20 L) was centrifuged to separate the mycelia from the supernatant. The extracts of the fermentation broth and the mycelia were combined after TLC analysis to yield crude extract (15.0 g). The residue was first subjected to column chromatography (CC) (silica gel, $CHCl_3$/MeOH 100:0, 50:1, 30:1, 10:1, and 5:1 (v/v)) to afford Fractions 1−5. Fr. 1 was separated by column chromatography on silica gel eluted with petroleum ether/EtOAc (60:1, 30:1, 10;1, 3;1, 1:1) to give five subfractions (Fr. 1.1−Fr. 1. 5). The subfraction Fr. 1.3 was eluted upon Sephadex LH-20 (methanol) to give four subfractions (Fr. 1.3.1−Fr. 1.3.4). The subfraction Fr.1.3.2 was further subjected to a Lichroprep RP-18 column with MeOH−H_2O (10−50%) to give compound **1** (5 mg). Fr. 1.3.3 was eluted upon Sephadex LH-20 (methanol) to afford compounds **2** and **3** (10 mg). Fr. 2 was fractioned by column chromatography on silica gel eluted with $CHCl_3$/MeOH (50:1, 20:1, 5:1) to give five subfractions (Fr. 2.1−Fr. 2.5). Fr. 2.3 was further subjected to column chromatography on silica gel eluted with petroleum ether/EtOAc (8:1) to afford compounds **6** and **14** (8 mg). Fr. 2.1 was fractioned by Lichroprep RP-18 column chromatography on a gradient eluted with MeOH−H_2O (20−100%) to give four subfractions (Fr. 2.3.1−Fr. 2.3.4). Fr. 2.3.1 was fractioned finally by Sephadex LH-20 (methanol) to afford compounds **4** and **5** (7 mg).

Paraverrucsin A (**1**): $[\alpha]_D^{25}$ − 42.30 (*c* 0.1, MeOH); HR-ESIMS m/z 237.1117 $[M + Na]^+$ (Calcd for $C_{11}H_{18}NaO_4$ 237.1103). ^1H NMR (600 MHz) and ^{13}C NMR (150 MHz) see in Table 1.

Paraverrucsin B (**2**), paraverrucsin C (**3**): HR-ESIMS m/z 223.0959 $[M + Na]^+$ (Calcd for $C_{10}H_{16}NaO_4$ 223.0946). ^1H NMR (600 MHz) and ^{13}C NMR (150 MHz) see in Table 1.

Paraverrucsin D (**4**), paraverrucsin E (**5**): HR-ESIMS m/z 249.0734 $[M + Na]^+$ (Calcd for $C_{11}H_{14}O_5Na$ 249.0739). ^1H NMR (600 MHz) and ^{13}C NMR (150 MHz) see in Table 2.

Paraverrucsin F (**6**): HR-ESIMS m/z 263.0901 $[M + Na]^+$ (Calcd for $C_{12}H_{16}O_5Na$ 263.0895). ^1H NMR (600 MHz) and ^{13}C NMR (150 MHz) see in Table 2.

NMR Computational Methods. The corresponding stable conformers were collected. The calculations in solution were carried out using the polarizable continuum model (PCM) for methanol (the solvent used experimentally). After this, compounds **1**−**6** were first optimized at the PCM/mPW1PW91/6−311 + G (d, p) level of theory, subsequently subjected to ^{13}C NMR calculations by using the gauge-independent atomic orbital (GIAO) method at the PCM/mPW1PW91/6−311 + G (d, p) level of theory for DP4+ calculations.[18] The computed chemical shifts of possible diastereomers of **1**−**6** were compared with the experimental values using DP4+ probability analyses.[19] The DP4+ analysis predicted the structure of **1**−**6**, leading to the unequivocal assignment of the configuration for **1**−**6**.

Antifeedant Bioassay against Silkworm Larvae. The antifeedant activities of compounds **2**−**13** were evaluated with the methods described in the literature.[20] These samples were diluted in acetone to afford the mother liquor with a concentration of 5 mg/mL. The samples (10 μL) were added to each mulberry leaf (1 cm × 1 cm) and spread wholly and air-dried at room temperature. Five mulberry leaves and 10 silkworm larvae were placed together in one 90 mm diameter Petri dish. The remaining leaf area of the treatment and the control were gauged separately after 24 h. The percent antifeedant index was calculated as following: antifeedant index (%) = $[(CK - T)/CK] \times 100$, where CK is the leaf area expended in the control, while *T* is the leaf area expended in the treatment.

Antifungal Assays. Four strains of plant pathogenic fungi (*Colletotrichum gloeosporioides*, *Didymella glomerata*, *Nigrospora oryzae*, and *Paraphaeosphaeria verruculosa*) were selected for the antimicrobial assay. The strains were cultivated in a sterile PDB broth medium. The test samples were dissolved in dimethyl sulfoxide (DMSO), and their final concentrations ranged from 512 to 1 μg/mL by using the twofold serial dilution method. The final capacity of each well was 0.1 mL. Samples (5 μL) of the metabolite solutions in dimethyl sulfoxide were added to 96-well plates. The wells containing

https://dx.doi.org/10.1021/acsomega.0c04548
ACS Omega 2020, 5, 30596−30602

metabolite-free cultures were applied as negative controls, and the wells containing nystatin (Aladdin Company, purity >99%) were used as the positive drugs. All experiments were repeated in triplicate. The wells containing test strains and diluted compounds were incubated at 28 °C (4 days) for fungi.

Cytotoxic Assay. The cytotoxicities of compounds **1**, **2**/**3**, **4**/**5**, **6**/**14** against HL-60, SMMC-7721, A-549, MCF-7, and SW480 were determined in vitro by the 3-(4,5-dimethylthiazol-2-yl)-5(3-carboxymethoxyphenyl)-2-(4-sulpopheny)-2*H*-tetrazolium (MTS) method. Cells were treated with different concentrations of compounds **1**, **2**/**3**, **4**/**5**, **6**/**14** for 48 h, following incubation with MTS solution for 2−4 h. The absorbance was measured using a microplate reader (Multiskan FC) at a wavelength of 490 nm. Cisplatin was used as a positive control.

CONCLUSIONS

In summary, six new polyketides (**1**−**6**) including paraverrucsin A−C (**1**−**3**) with a novel decarboxylated trichocladinol skeleton were first isolated from rhizospheric *Paraphaeosphaeria verruculosa*. Paraverrucsins B/C, D/E, F/trichocladinol B, **8**, and **9** exhibited insect antifeedant activities. Most compounds showed antifungal activities against phytopathogenic fungi. The interaction of *P. verruculosa* and its host plant *Dendrobium officinale* from coculture could bring about the enhancements of antifeedant and antiphytopathogenic activities. New compounds (**1**, **2**/**3**, **4**/**5**, **6**/**14**) exhibited selected cytotoxicity against human colon cancer cells SW480.

ASSOCIATED CONTENT

Supporting Information

The Supporting Information is available free of charge at https://pubs.acs.org/doi/10.1021/acsomega.0c04548.

Experimental and calculated NMR spectra of **1**−**6**; ^{1}H and ^{13}C NMR; HSQC, HMBC, ^{1}H-^{1}H COSY, NOESY, and HR-ESIMS spectra of compounds **1**−**6**; the antifeedant activities of **9** against silkworm larvae (PDF)

AUTHOR INFORMATION

Corresponding Authors

Ya-Bin Yang − *Functional Molecules Analysis and Biotransformation Key Laboratory of Universities in Yunnan Province, and Key Laboratory of Medicinal Chemistry for Natural Resource, Ministry Education and Yunnan Province, School of Chemical Science and Technology, Yunnan University, Kunming 650091, China*; orcid.org/0000-0001-5509-4559; Email: ybyang@ynu.edu.cn

Zhong-Tao Ding − *Functional Molecules Analysis and Biotransformation Key Laboratory of Universities in Yunnan Province, and Key Laboratory of Medicinal Chemistry for Natural Resource, Ministry Education and Yunnan Province, School of Chemical Science and Technology, Yunnan University, Kunming 650091, China*; orcid.org/0000-0002-7860-060X; Email: ztding@ynu.edu.cn

Authors

Ming Hu − *Functional Molecules Analysis and Biotransformation Key Laboratory of Universities in Yunnan Province, and Key Laboratory of Medicinal Chemistry for Natural Resource, Ministry Education and Yunnan Province, School of Chemical Science and Technology, Yunnan University, Kunming 650091, China*

Xue-Qiong Yang − *Functional Molecules Analysis and Biotransformation Key Laboratory of Universities in Yunnan Province, and Key Laboratory of Medicinal Chemistry for Natural Resource, Ministry Education and Yunnan Province, School of Chemical Science and Technology, Yunnan University, Kunming 650091, China*

Cui-Fang Wang − *Functional Molecules Analysis and Biotransformation Key Laboratory of Universities in Yunnan Province, and Key Laboratory of Medicinal Chemistry for Natural Resource, Ministry Education and Yunnan Province, School of Chemical Science and Technology, Yunnan University, Kunming 650091, China*

Tong-De Zhao − *Functional Molecules Analysis and Biotransformation Key Laboratory of Universities in Yunnan Province, and Key Laboratory of Medicinal Chemistry for Natural Resource, Ministry Education and Yunnan Province, School of Chemical Science and Technology, Yunnan University, Kunming 650091, China*

Dai-Li Wang − *Functional Molecules Analysis and Biotransformation Key Laboratory of Universities in Yunnan Province, and Key Laboratory of Medicinal Chemistry for Natural Resource, Ministry Education and Yunnan Province, School of Chemical Science and Technology, Yunnan University, Kunming 650091, China*

Complete contact information is available at: https://pubs.acs.org/10.1021/acsomega.0c04548

Author Contributions

§M.H. and X.Q.Y. contributed equally to this work.

Notes

The authors declare no competing financial interest.

ACKNOWLEDGMENTS

This project was supported by the National Natural Science Foundation of China (81560571, 81660582, and 81960640), the projects of the Yunling Scholars of Yunnan Province and Donglu Scholars of Yunnan University, and the Program for Changjiang Scholars and Innovative Research Team in University (IRT-17R94). The Yunnan University's Research Innovation Fund for Graduate Students (2019z047, 2019188) is also acknowledged.

REFERENCES

(1) Berini, F.; Katz, C.; Gruzdev, N.; Casartelli, M.; Tettamanti, G.; Marinelli, F. Microbial and viral chitinases: Attractive biopesticides for integrated pest management. *Biotechnol. Adv.* **2018**, *36*, 818−838.

(2) Johansen, A.; Olsson, S. Using phospholipid fatty acid technique to study short-term effects of the biological control agent *Pseudomonas fluorescens* DR54 on the microbial microbiota in barley rhizosphere. *Microb. Ecol.* **2005**, *49*, 272−281.

(3) Zheng, H.; Wang, X.; Chen, L.; Wang, Z.; Xia, Y.; Zhang, Y.; Wang, H.; Luo, X.; Xing, B. Enhanced growth of halophyte plants in biochar-amended coastal soil: roles of nutrient availability and rhizosphere microbial modulation. *Plant Cell Environ.* **2018**, *41*, 517−532.

(4) Hubbard, C. J.; Li, B.; Mcminn, R.; Brock, M. T.; Maignien, L.; Ewers, B. E.; Kliebenstein, D.; Weinig, C. The effect of rhizosphere microbes outweighs host plant genetics in reducing insect herbivory. *Mol. Ecol.* **2019**, *28*, 1801−1811.

(5) Anderson, A. J.; Kim, Y. C. Biopesticides produced by plant probiotic *Pseudomonas chlororaphis* isolates. *Crop Prot.* **2018**, *105*, 62−69.

(6) Pieczul, K.; Perek, A. First report of *Paraphaeosphaeria recurvifoliae* on *Yucca filamentosa* in western Poland. *Plant Dis.* **2016**, *100*, 1018.
(7) Suga, T.; Shiina, M.; Asami, Y.; Iwatsuki, M.; Yamamoto, T.; Nonaka, K.; Masuma, R.; Matsui, H.; Hanaki, H.; Iwamoto, S.; Onodera, H.; Shiomi, K.; Ōmura, S. Paraphaeosphaeride D and berkleasmin F, new circumventors of arbekacin resistance in MRSA, produced by *Paraphaeosphaeria* sp. TR-022. *J. Antibiot.* **2016**, *69*, 605−610.
(8) Dina, B.; Mamtaj, S. D. Endophytic microorganisms: colonization, plant-microbe interaction, diversity and their Bioprospecting. *Res. J. Biotechnol.* **2020**, *15*, 151−179.
(9) Chen, S.; Ren, F.; Niu, S.; Liu, X.; Che, Y. Dioxatricyclic and oxabicyclic polyketides from *Trichocladium opacum*. *J. Nat. Prod.* **2014**, *77*, 9−14.
(10) Guo, H.; Sun, B.; Gao, H.; Niu, S.; Liu, X.; Yao, X.; Che, Y. Trichocladinols A−C, Cytotoxic metabolites from a cordyceps-colonizing ascomycete *Trichocladium opacum*. *Eur. J. Org. Chem.* **2009**, *32*, 5525−5530.
(11) Kock, I.; Krohn, K.; Egold, H.; Draeger, S.; Schulz, B.; Rheinheimer, J. New massarilactones, massarigenin E, and coniothyrenol, isolated from the endophytic fungus *Coniothyrium* sp. from *Carpobrotus edulis*. *Eur. J. Org. Chem.* **2007**, *2007*, 2186−2190.
(12) Lin, Y.; Wu, X.; Deng, Z.; Wang, J.; Zhou, S.; Vrijmoed, L. L. P.; Jones, E. B. G. The metabolites of the mangrove fungus *Verruculina enalia* No. 2606 from a salt lake in the Bahamas. *Phytochemistry* **2002**, *59*, 469−471.
(13) Krohn, K.; Ullah, Z.; Hussain, H.; Florke, U.; Schulz, B.; Draeger, S.; Pescitelli, G.; Salvadori, P.; Antus, S.; Kurtan, T. Massarilactones, E-G, new metabolites from the endophytic fungus *Coniothyrium* sp., associated with the plant *Artimisia maritima*. *Chirality* **2007**, *19*, 464−470.
(14) Xu, Y.-M.; Mafezoli, J.; Oliveira, M. C. F.; U'Ren, J. M.; Arnold, A. E.; Gunatilaka, A. A. L. Anteaglonialides A−F and palmarumycins CE1−CE3 from *Anteaglonium* sp. FL0768, a fungal endophyte of the Spikemoss *Selaginella arenicola*. *J. Nat. Prod.* **2015**, *78*, 2738−2747.
(15) Krohn, K.; Michel, A.; Flörke, U.; Aust, H. J.; Draeger, S.; Schulz, B. Biologically active metabolites from fungi, 4. palmarumycins CP1−CP4 from *Coniothyrium palmarum*: isolation, structure elucidation, and biological activity. *Liebigs Ann. Chem.* **1994**, *11*, 1093−1097.
(16) Macías-Rubalcava, M. L.; Sobrino, M. E. R.-V.; Meléndez-González, C.; Hernández-Ortega, S. Naphthoquinone spiroketals and organic extracts from the endophytic fungus *Edenia gomezpompae* as potential herbicides. *J. Agric. Food Chem.* **2014**, *62*, 3553−3562.
(17) Oh, H.; Swenson, D. C.; Gloer, J. B.; Shearer, C. A. New bioactive rosigenin analogues and aromatic polyketide metabolites from the freshwater aquatic fungus *Massarina tunicata*. *J. Nat. Prod.* **2003**, *66*, 73−79.
(18) Wolinski, K.; Hinton, J. F.; Pulay, P. Efficient implementation of the gauge-independent atomic orbital method for NMR chemical shift calculations. *J. Am. Chem. Soc.* **1990**, *112*, 8251−8260.
(19) Liu, H.; Wang, X.; Shi, Q.; Li, L.; Zhang, Q.; Wu, Z.-L.; Huang, X.-J.; Zhang, Q.-W.; Ye, W.-C.; Wang, Y.; Shi, L. Dimeric diarylheptanoids with neuroprotective activities from rhizomes of *Alpinia officinarum*. *ACS Omega* **2020**, *5*, 10167−10175.
(20) Wu, H.; Liu, T.; Lian, Y.; Wang, W. Two new eremophilenolides from the roots of *Ligulariopsis shichuana* and their anti-phytopathogenic fungal and antifeedant activities. *Nat. Prod. Res.* **2019**, *33*, 1442−1448.

https://dx.doi.org/10.1021/acsomega.0c04548
ACS Omega 2020, 5, 30596−30602